

# SIMULATED BEAM-BEAM LIMIT FOR CIRCULAR HIGGS FACTORIES

K. Ohmi, KEK-ACCL, 1-1 Oho, Tsukuba, 305-0801, Japan  
F. Zimmermann, CERN-ABP, Geneva, CH-1211, Switzerland

## Abstract

We report simulation studies of the beam-beam limit for two proposed circular  $e^+e^-$  Higgs factories with circumference of 27 and 80 km, respectively, called LEP3 and TLEP. In particular we investigate the dependence of the steady-state luminosity and transverse beam sizes on the synchrotron tune (or momentum compaction factor) and on the betatron tunes, as well as the consequences of the strong radiation damping and the implications of the large hourglass effect.

## INTRODUCTION

In our beam-beam studies we consider parameters of LEP3 and TLEP for Higgs-production running at 240 GeV c.m. [1] which are summarized in Table 1. A high luminosity of  $10^{34}$  cm $^{-2}$ s $^{-1}$  or  $5 \times 10^{34}$  cm $^{-2}$ s $^{-1}$  per IP is realized, despite the small number of bunches, thanks to a low  $\beta_y^*$  and short bunch length. In the following we consider two interaction points (IPs), though LEP3 and TLEP could in principle accommodate four IPs (like the previous LEP collider).

We investigate the classical beam-beam effects in these circular Higgs factories using a strong-strong simulation code (BBSS) as well as a weak-strong code (BBWS) for validation of the results. Beamstrahlung (synchrotron radiation during collision) is not included.

Table 1: Parameters of LEP3 and TLEP-H [1]

	LEP3	TLEP-H
beam energy (GeV)	120	120
circumference (km)	26.7	80
number of bunches / beam	4	80
number of IPs	2	2
bunch population ( $10^{12}$ )	1	1
geometric emittance ( $x/z$ , nm)	25/0.1	9.4/0.05
beta* ( $x/z$ , mm)	200/1	200/1
momentum compaction factor	$8.1 \times 10^{-5}$	$1 \times 10^{-5}$
RF voltage (GV)	12	6
rms bunch length (mm)	2.3	1.7
synchrotron tune	0.348	0.117
rad. damping time ( $x/z$ , turn)	30/23	76/110
beam-beam parameter ( $\xi_{x/y}/IP$ )	0.09/0.08	0.1/0.1
luminosity/IP ( $10^{34}$ cm $^{-2}$ s $^{-1}$ )	1.07	4.90

## 3-D BEAM-BEAM INTERACTION

The vertical beta function at the IP is smaller than the bunch length. Therefore the beam-beam force varies significantly along the bunch. As a consequence the three-dimensional beam-beam effect should be taken into account in the simulation. The longitudinal variation is taken into account by slicing a bunch and evaluating the

collisions slice-by-slice. Specifically, a bunch is sliced into 16 pieces and is represented by 1,000,000 macro-particles in the simulation. Macro-particles travel between slices as a result of their synchrotron motion. The transverse beam-beam force should change smoothly along  $z$ . In our model a macro-particle  $j$  at location  $z_j$  collides with a slice  $c$  of the opposite bunch characterized by the center of mass  $z_c$  at the location  $s_{jc}=(z_j-z_c)/2$ . The potential of the slice has to be evaluated at the coordinate  $s_{jc}$  for every macro-particle and slice. To reduce the computation time, the potential is evaluated at  $s_f$  and  $s_b$ , where  $s_f=(z_f-z_c)/2$  and  $s_b=(z_b-z_c)/2$  are collision point with front face ( $z_f$ ) and back face ( $z_b$ ) of the slice containing the macro-particle, and is interpolated to  $s_j$  as

$$\phi(s_j) = \phi(s_b) + \frac{\phi(s_f) - \phi(s_b)}{s_f - s_b}(s_j - s_b) \quad (1)$$

Figure 1 shows a schematic view of the collision and the interpolated potential. Black and red lines are interpolated and non-interpolated, respectively. The large steps in the transverse potential between longitudinal slices for the case without interpolation induce an unphysical luminosity degradation. Small steps between slices in the interpolated case are due to beam-beam disruption.

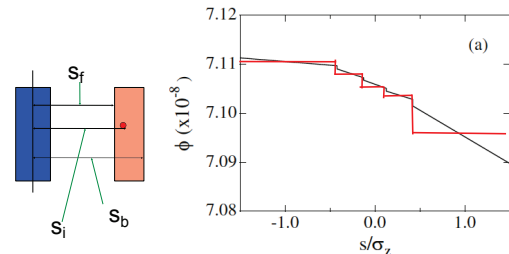


Figure 1: Schematic view of collision and interpolated potential (left), and potential along  $s$  for an example with 5 slices (right) [2].

Since the transverse beam aspect ratio at the collision point is large, namely  $\sigma_x/\sigma_y=200-220$ , the integrated Green function [3,4] is used to calculate the potential.

## SIMULATION RESULTS

The macro-particles are tracked over 1000 turns, which corresponds to 33 and 13 radiation damping times for LEP3 and TLEP-H, respectively. The simulated luminosity and beam sizes are plotted turn by turn, in order to demonstrate that a steady state of luminosity and beam size is obtained.

In electron positron colliders with a single interaction point the luminosity performance is generally expected to be high at an operating point near  $(\nu_x, \nu_y)=(0.52, 0.58)$  [5]. Since we here consider cases of two interaction points,

we first examine the beam-beam performance at the 2-IP equivalent operating point with fractional tunes of  $(\nu_x, \nu_y) = (0.52, 0.58) \times 2 = (0.04, 0.16)$ .

Figure 2 presents the simulated luminosity evolution for the collision of single bunches in LEP3 (top) and TLEP-H (bottom). The luminosity varies in the early stage (~30 turns) and then acquires steady-state values of  $2.4 \times 10^{33} \text{ cm}^{-2} \text{ s}^{-1}$  and  $0.8 \times 10^{33}$ , respectively. The green lines correspond to the single-bunch design luminosities,  $10.7 \times 10^{33} / 4 = 2.68 \times 10^{33} \text{ cm}^{-2} \text{ s}^{-1}$  and  $49 \times 10^{33} / 80 = 0.61 \times 10^{33}$  for LEP3 and TLEP-H, respectively. The luminosity is somewhat (10%) lower than the design for LEP3, while it is slightly higher than the design (~30%) for TLEP-H. Steady-state beam sizes are  $(\sigma_x, \sigma_y) = (55, 0.64) \mu\text{m}$  for LEP3, to be compared with the design values of  $(71, 0.32) \mu\text{m}$  for LEP3, while the simulated steady-state sizes are  $(35, 0.27) \mu\text{m}$  for TLEP-H with a design of  $(43, 0.22) \mu\text{m}$ . The horizontal beam size is smaller than the design due to the dynamic beta effect for a horizontal tune close to a half integer/IP. The vertical beam size is enlarged, especially for LEP3. This vertical beam-size increase is responsible for the observed luminosity degradation.

Figure 3 shows the steady-state LEP3 luminosity for an increasing bunch population. The design luminosity is reached at 10% higher current is necessary. The specific luminosity, i.e. the luminosity normalized to the product of the bunch populations, degrades for increasing bunch population. This implies that dynamic beam-beam effects are noticeable for the parameter range considered.

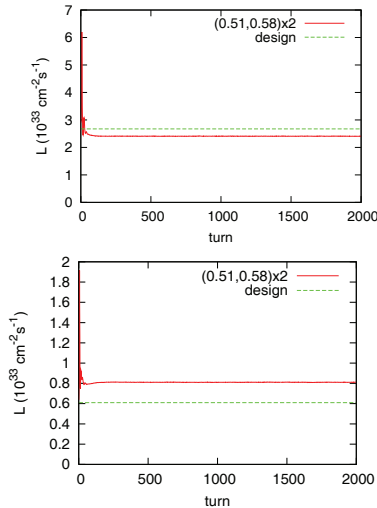


Figure 2: Luminosity evolution for LEP3 (top) and TLEP-H (bottom) at the operating point  $(\nu_x, \nu_y) = (0.51, 0.58) \times 2$ .

### Operating Point

The luminosity performance depends on the operating point in tune space. Normally, the simulated luminosity is higher than the geometrical value for the operating point  $(\nu_x, \nu_y) = (0.52, 0.58) \times 2 = (0.04, 0.16)$  considered above, because of the dynamic beta in the horizontal and the high integrability in the vertical plane [5]. However, for

LEP3 the luminosity is lower than the design. The operating point was varied to examine its effect on the luminosity. Figure 4 shows the steady-state luminosity for LEP3 and TLEP-H for a tune survey in the proximity of the original working point. In LEP3 the luminosity strongly depends on the vertical tune, but only shows a weak dependence on the horizontal tune. By contrast, for TLEP-H a strong sensitivity to the horizontal tune is seen for a bad choice of vertical tune, i.e. for  $\nu_y = 0.1$  and  $0.12$ .

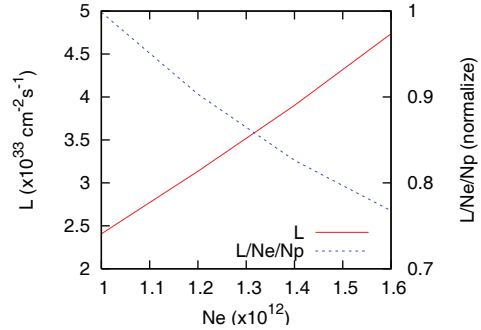


Figure 3: Steady-state luminosity and specific luminosity (normalized by bunch population product) for LEP3 as a function of bunch population.

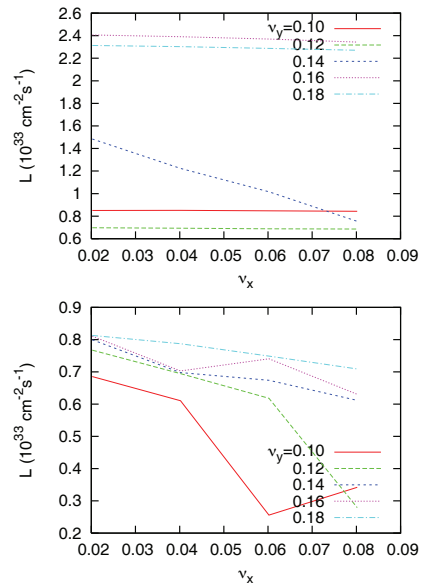


Figure 4: Steady-state luminosity for LEP3 (top) and TLEP-H near integer tune (bottom). The design values are  $2.67$  and  $0.61 \times 10^{33} \text{ cm}^{-2} \text{ s}^{-1}$ /bunch, respectively.

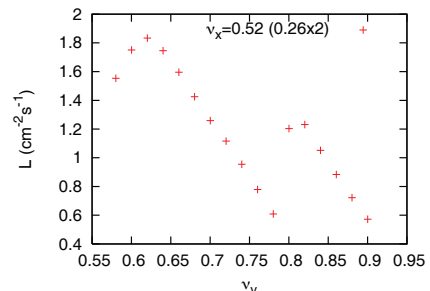


Figure 5: Simulated steady-state luminosity for LEP3 over another, wide vertical tune area.

It may be difficult to achieve the design luminosity in other areas of tune space. Figure 5 shows the steady-state luminosity for  $\nu_x=0.52$ . The luminosity does not exceed  $2 \times 10^{33} \text{ cm}^{-2} \text{ s}^{-1}$  / bunch for  $0.55 < \nu_y < 0.90$ .

### Synchrotron Tune and Hourglass Effect

The synchrotron tune is higher than for ordinary electron storage rings, due to the high RF voltage needed to compensate the large energy loss from synchrotron radiation. The hourglass effect is strong, because  $\sigma_z \sim 2\beta_y^*$ . The hourglass effect and the large synchrotron tune may conspire, from the beam-dynamics point of view.

Figure 6 displays the simulated luminosity as a function of the synchrotron tune. The left and right plots refer to rms bunch lengths of 2.3 mm (design) and 1 mm, respectively. At  $\nu_s < 0.2$  the luminosity is higher than the geometrical value, because of the horizontal dynamic beta effect. Increasing the synchrotron tune, the luminosity degrades in both cases. The degradation is stronger for the longer bunch length. In the limit of zero bunch length, the dependence on the synchrotron tune should disappear. In the left picture, also simulations with a larger number of slices (20) are compared with the default number (16). Figure 7 shows results for the same situation using a weak-strong simulation. At low values of synchrotron tune, the luminosity is lower than in the strong-strong simulation, because the dynamic beta is mild in the weak-strong simulation. However, the luminosity degradation at high synchrotron tunes is reproduced. The behavior of this degradation indicates a resonance effect.

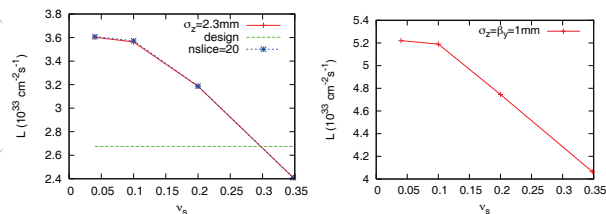


Figure 6: Simulated steady-state luminosity for LEP3 as a function of synchrotron tune, for rms bunch lengths of 2.3 mm (left) and 1 mm (right).

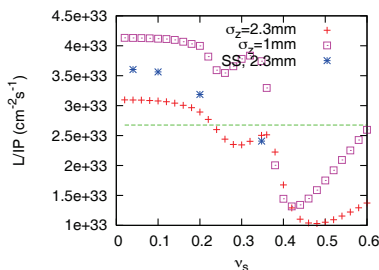


Figure 7: Steady-state LEP3 luminosity as a function of synchrotron tune obtained from a weak-strong simulation.

Figure 8 shows results of a frequency map analysis [6,7]. The synchrotron motion affects the transverse beam-beam force, while the longitudinal beam-beam force only weakly affects the synchrotron motion. Our interest is in the behavior of  $J_y$ - $J_z$ - $\nu_y$  space. Diffusion indices ( $D$ ) [6] in the  $J_z$ - $\nu_y$  space for  $\nu_s=0.02$  and  $0.34$  are depicted in pictures (a) and (b), respectively.  $J_y$ - $\nu_y$  plot for  $\nu_s=0.34$  is in (c).

6th, 8th, and 10th order are seen. These resonances merge at large synchrotron amplitude,  $z > \sigma_z$ . Also the vertical tune shift as a function of vertical amplitude is shown in picture (c), as line with low diffusion index. The diffusion index mainly depends on the synchrotron amplitude.

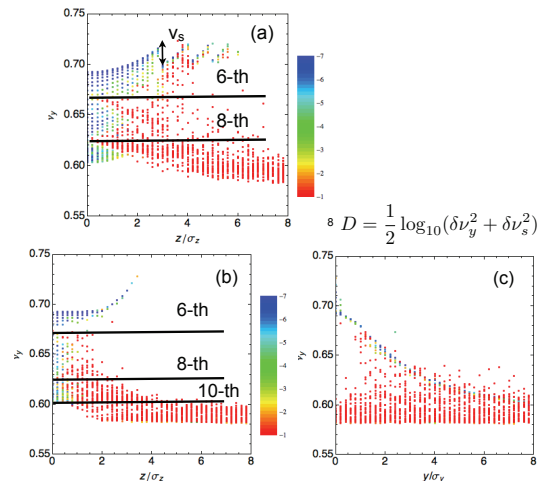


Figure 8: FMA analysis for  $y$ - $z$  motion for  $\nu_y=0.16$ . Diffusion index ( $D$ ) in  $J_z$ - $\nu_y$  space for  $\nu_s=0.02$  and  $0.34$  are depicted in pictures (a) and (b), respectively.  $J_y$ - $\nu_y$  plot for  $\nu_s=0.34$  is in (c).

## SUMMARY AND CONCLUSIONS

We simulated the beam-beam effect and luminosity performance for two proposed storage-ring based Higgs factories. Considering, with 2 IPs, a tune working point of  $(\nu_x, \nu_y)=(0.52, 0.58) \times 2=(0.04, 0.16)$ , for LEP3 the design luminosity is achieved with a current 10% higher than the design; for TLEP-H it is exceeded at the design current. The simulated luminosity is degraded by the high synchrotron tune. This degradation is more serious at other operating points. Future studies are planned in wider areas of tune space and with varying number of IPs.

## ACKNOWLEDGMENTS

We thank Katsunobu Oide for a helpful question at the first LEP3/TLEP mini-workshop. These studies were supported, in parts, by the EC FP7 RI project EuCARD, grant agreement no. 227579, and by the Large Scale Simulation Program No.12/13-06 of KEK.

## REFERENCES

- [1] A. Blondel et al., submission no. 173, Open Symposium – European Strategy Preparatory Group, 10-12 September 2012, Cracow, Poland
- [2] K. Ohmi et al., Phys. Rev. ST-AB, 7 104401(2004).
- [3] K. Ohmi, Phys. Rev. E62, 7287 (2000).
- [4] J. Qiang et al., Phys. Rev. ST-AB 9, 044204 (2006).
- [5] K. Ohmi et al., Proceedings of EPAC06, MOPLS032.
- [6] L. Nadolski, J. Laskar, Phys. Rev. ST-AB, 6 (2003), 114801.
- [7] J. Laskar, Icarus 88, 266 (1990)